Quantitative Analysis of Binding of Single-Stranded DNA by *Escherichia coli* DnaB Helicase and the DnaB·DnaC Complex†

Subhasis B. Biswas*,‡ and Esther E. Biswas-Fiss‡,§

Department of Molecular Biology, School of Medicine and Graduate School of Biomedical Sciences, University of Medicine and Dentistry of New Jersey, Stratford, New Jersey 08084, and Program in Biotechnology, Department of Bioscience Technologies, Thomas Jefferson University, Philadelphia, Pennsylvania 19107

Received January 19, 2006; Revised Manuscript Received July 10, 2006

ABSTRACT: DnaB helicase is responsible for unwinding duplex DNA during chromosomal DNA replication and is an essential component of the DNA replication apparatus in *Escherichia coli*. We have analyzed the mechanism of binding of single-stranded DNA (ssDNA) by the DnaB·DnaC complex and DnaB helicase. Binding of ssDNA to DnaB helicase was significantly modulated by nucleotide cofactors, and the modulation was distinctly different for its complex with DnaC. DnaB helicase bound ssDNA with a high affinity [$K_d = (5.09 \pm 0.32) \times 10^{-8}$ M] only in the presence of ATPγS, a nonhydrolyzable analogue of ATP, but not other nucleotides. The binding was sensitive to ionic strength but not to changes in temperature in the range of 30−37 °C. On the other hand, ssDNA binding in the presence of ADP was weaker than that observed with ATPγS, and the binding was insensitive to ionic strength. DnaC protein hexamerizes to form a 1:1 complex with the DnaB hexamer and loads it onto the ssDNA by forming a $DnaB_6$·$DnaC_6$ dodecameric complex. Our results demonstrate that the $DnaB_6$·$DnaC_6$ complex bound ssDNA with a high affinity [$K_d = (6.26 \pm 0.65) \times 10^{-8}$ M] in the presence of ATP, unlike the DnaB hexamer. In the presence of ATPγS or ADP, binding of ssDNA by the $DnaB_6$·$DnaC_6$ complex was a lower-affinity process. In summary, our results suggest that in the presence of ATP in vivo, the $DnaB_6$·$DnaC_6$ complex should be more efficient in binding DNA as well as in loading DnaB onto the ssDNA than DnaB helicase itself.

DnaB helicase of *Escherichia coli* is the primary replicative DNA helicase that unwinds duplex DNA during replication of the *E. coli* genome (*1*, *2*). In the replication fork, unwinding of the DNA duplex by DnaB allows DNA primase (DnaG) to initiate synthesis of primers that are extended to Okazaki fragments (*1*, *3*, *4*). DnaB helicase is a homohexamer comprised of 52 kDa subunits (*5*). It unwinds duplex DNA in a 5′ → 3′ direction with high processivity, using the energy of nucleotide hydrolysis (*2*, *6*−*11*). The *E. coli* single-stranded DNA (ssDNA)[1] binding protein (SSB) modulates DnaB DNA-dependent ATPase activity and makes it specific for forked duplex structures and stimulates its helicase activity (*6*, *12*).

DnaC protein is a 29 kDa protein that hexamerizes to form a 1:1 complex with the DnaB hexamer and loads it onto the ssDNA generated by localized DNA melting at *ori*C by DnaA protein (*13*−*16*). We have shown earlier that the DnaC protein first forms a $DnaB_6$·$DnaC_6$·ATP inactive ternary complex in which the ATPase activity is attenuated (*17*). In bacteriophage λ genomic DNA replication, λP protein appears to act in a similar manner, leading to a $DnaB_6$·λP_6·ATP dead-end ternary complex (*2*, *18*). The release of DnaC or λP from the ternary complex is required for the rejuvenation of the DnaB ATPase and its coupled DNA helicase activities. Therefore, the $DnaB_6$·$DnaC_6$·ATP ternary complex interacts first with ssDNA before activation of its ATPase and DNA helicase activities. Studies by Learn et al. (*19*) suggested alterations in the DNA binding properties of DnaB helicase in the presence of DnaC or λP proteins. Therefore, quantitative analysis of the ssDNA binding properties of the DnaB protein complex with DnaC protein is required to understand the dynamics of DNA binding during initiation of DNA replication in *E. coli*. Arai and Kornberg (*6*) first studied the ssDNA binding by DnaB helicase. The authors reported efficient ssDNA binding by the DnaB helicase in the presence of a nonhydrolyzable analogue of ATP, ATPγS, which was inhibited by ADP and deoxynucleotides. Jezeweska et al. (*20*−*22*) reported dissociation constants for binding of DnaB helicase to ssDNA. The dissociation constant for DnaB bound to synthetic poly(dϵA) was found to be low (7.69 μM) (*21*). Using a separate method, macromolecular competition titration, with other polynucleotides such as poly(dA), poly(dT), etc., a wide range of dissociation constants were reported (*20*, *22*). The ssDNA binding properties of the DnaB·DnaC complex remain unknown. Therefore, evaluation of the mechanism of DNA

† This work was supported by a grant from the National Institute of General Medical Sciences, National Institutes of Health (GM36002), and funds from the University of Medicine and Dentistry of New Jersey.

* To whom correspondence should be addressed. Telephone: (856) 566-6270. Fax: (856) 566-6291. E-mail: biswassb@umdnj.edu.

‡ University of Medicine and Dentistry of New Jersey.

§ Thomas Jefferson University.

[1] Abbreviations: Tris, tris(hydroxymethyl)aminomethane; BSA, bovine serum albumin; EDTA, ethylenediaminetetraacetic acid; ssDNA, single-stranded DNA; mA, millianisotropy; DTT, dithiothreitol; wt, wild type.

10.1021/bi060118d CCC: $33.50
Published on Web 08/31/2006

binding by the DnaB·DnaC complex and DnaB helicase under identical conditions would be necessary to understand the role of this complex in vivo.

In this study, interactions of the DnaB hexamer and $DnaB_6$·$DnaC_6$ complex with ssDNA were analyzed by measuring changes in the anisotropy of a fluorescent oligonucleotide ligand upon formation of the protein·DNA complex (*23*−*25*). Fluorescence anisotropy permits acquisition of data under a variety of physical and equilibrium conditions, and it does not require separation of the bound and free ligands (*25*−*28*). ssDNA binding was assessed under different physical conditions, and the thermodynamic parameters of DNA binding were determined. This analytical strategy has been useful in studying protein−DNA interactions involving a variety of DNA binding proteins, including binding of the estrogen receptor to estrogen responsive elements, binding of the tryptophan repressor to the tryptophan operator, and binding of *E. coli* DNA primase to ssDNA (*23*, *27*, *29*, *30*).

MATERIALS AND METHODS

Nucleic Acids and Other Reagents. Labeled and unlabeled oligonucleotides were both purchased from Sigma-Genosys and Fisher Chemicals Inc. (Pittsburgh, PA). The labeled oligonucleotide, fluorescein-oligo$(dT)_{25}$ [Fl-$(dT)_{25}$], that was used was covalently linked with the fluorescein probe at the 5′ end. The following unlabeled oligonucleotides were used in this study: oligo$(dT)_{25}$, oligo$(dT)_{20}$, oligo$(dT)_{15}$, oligo$(dT)_{10}$, and oligo$(dT)_6$. All other reagents used in this study were ACS reagent or spectroscopy grade and obtained from Aldrich Chemical Co. (Milwaukee, WI). HPLC grade water was obtained from Fisher Chemicals and analyzed for low autofluorescence.

Buffers. Buffer A consisted of 25 mM Tris-HCl (pH 7.5), 5 mM $MgCl_2$, and 10% glycerol. Buffer B consisted of 25 mM Tris-HCl (pH 7.9), 10% sucrose, and 250 mM NaCl. Buffer C, used for anisotropy studies, consisted of 20 mM Tris-HCl (pH 7.5), 5 mM $MgCl_2$, and 10% glycerol, and KCl as indicated.

DnaB Helicase Expression and Purification. DnaB helicase was purified from an *E. coli* BL21(DE3) strain harboring the pET29b-DnaB expression plasmid following the published procedure (*31*, *32*). *E. coli* cells harboring the recombinant plasmid were grown with shaking at 37 °C to an OD_{600} of 0.4. IPTG was added to a final concentration of 0.10 mM, and incubation with shaking was continued for an additional 4 h at 37 °C. The cells were harvested by centrifugation for 10 min at 5000*g*, then resuspended in 2.5% of the original culture volume of buffer B at 4 °C, and stored at −80 °C until further use.

Extraction of the induced cells was conducted as previously described (*31*). DnaB protein was precipitated from the cell extract using 0.18 g/mL ammonium sulfate. The precipitated protein was resuspended in buffer A_0, and its ionic strength was adjusted to that of buffer A_{100} (buffer A with 100 mM NaCl) by dilution with buffer A_0. The protein was loaded on a POROS HQ column (Applied Biosystems Inc., Foster City, CA) equilibrated with buffer A_{100}. The protein was eluted using a linear gradient of 20 mL each of buffers A_{100} and A_{500} with a flow rate of 1 mL/min. The peak fractions were identified by Western blotting using a DnaB specific antibody, collected, and concentrated by ammonium sulfate precipitation. The purified DnaB protein was essentially homogeneous, greater than 98% pure, as analyzed by SDS−PAGE. The concentration of purified DnaB helicase was determined by UV absorption at 280 nm using a molar extinction coefficient of 2.9×10^4 (*32*).

DnaC Protein Expression and Purification. DnaC protein was expressed and purified as described previously (*13*). The $DnaB_6$·$DnaC_6$ complex was prepared by mixing purified DnaB and DnaC proteins and separating the $DnaB_6$·$DnaC_6$ complex from free DnaB and DnaC by gel filtration as described previously (*15*).

Steady-State *Fluorescence Measurements.* Fluorescence experiments were performed using a Fluorolog-2 spectrofluorometer (Jobin Yvon Horiba Inc., Edison, NJ), and measurements were taken in an L-format configuration of excitation and emission channels. Excitation and emission slits were adjusted to 8 and 4 nm, respectively, for all anisotropy measurements. The samples were excited at 488 nm, and the fluorescence anisotropy was measured at 540 nm, where minimal variation in the total fluorescence intensity was observed. The fluorescein-labeled oligonucleotide, Fl-$(dT)_{25}$, was diluted in buffer C to a concentration of 3×10^{-9} M and titrated with DnaB helicase at concentrations ranging from 3×10^{-9} to 1×10^{-6} M under different salt conditions or at different temperatures as indicated. The temperature was maintained by using a thermostat attached to the cell chamber. Anisotropy values were expressed as millianisotropy (mA) (anisotropy divided by 1000). The standard deviation for the anisotropy values was <0.005. The anisotropy reading for each titration point was taken three times for 10 s and averaged. The total fluorescence intensity did not change significantly with an increase in the DnaB concentration. Therefore, fluorescence lifetime changes, or the scattered excitation light, did not affect the anisotropy measurements.

Anisotropy (A) is defined as

$$A = (I_{vv} - GI_{vh})/(I_{vv} + 2GI_{vh}) \quad (1)$$

where G is the instrumental correction factor for the fluorometer and it is defined by

$$G = I_{hv}/I_{hh}$$

and I_{vv}, I_{vh}, I_{hv}, and I_{hh} represent the fluorescence signal for excitation and emission with the polarizers set at (0^0, 0^0), (0^0, 90^0), (90^0, 0^0), and (90^0, 90^0), respectively (*33*).

In general, the labeled oligonucleotide was diluted to 3 nM using buffer B. DnaB helicase was added in small amounts, and anisotropy was measured after incubation for 5 min after each addition. The interaction of DnaB helicase with labeled oligonucleotide can be represented as follows:

$$R + P \leftrightarrow RP \quad (2)$$

where R is the ligand, i.e., labeled oligonucleotides, and P is DnaB helicase, concentrations of which were varied during titration.

At equilibrium, K_a, the equilibrium association constant, can be given as

$$K_a = [RP]/[R][P] \quad (3)$$

$$K_a[R][P] = [RP] \quad (4)$$

The fraction of binding sites occupied can be represented as

$$f = (\text{occupied binding sites})/(\text{total binding sites}) = [RP]/([R] + [RP]) \quad (5)$$

Substituting for [RP] and rearranging the equation, we obtain

$$f = K_a \cdot P/(1 + K_a \cdot P) \quad (6)$$

$$f = [P]/([P] + 1/K_a) \quad (7)$$

Similarly, equilibrium dissociation constant K_d ($=1/K_a$) can be expressed as

$$f = [P]/([P] + K_d) \quad (8)$$

When $f = 0.5$

$$K_d = [P] \quad (9)$$

Thus, K_d can be further defined as the protein concentration at which half of the sites are occupied when the ligand concentration is constant, as in the present case, or the ligand concentration at which half of the sites are occupied when the protein concentration is constant. Nonlinear regression analysis of the anisotropy data was carried out using Prism, version 3.03 (GraphPad Software Inc., San Diego, CA), and the concentrations of DnaB helicase required to bind 50% of oligonucleotides (EC_{50} values) were computed using the following equation:

$$Y = A_{min} + (A_{max} - A_{min})/[1 + 10^{(X_0 - X)n_{app}}] \quad (10)$$

where A_{min} and A_{max} are the anisotropy values at the bottom and top plateaus, respectively, X represents the log of protein concentration, X_0 is the X value when the response is halfway between the top and the bottom, and n_{app} is the Hill coefficient.

Oligonucleotide Challenge Assays. Challenge experiments were used to compare the binding affinities of oligonucleotides differing in size. The preformed DnaB helicase·Fl-$(dT)_{25}$ complex was titrated with unlabeled oligonucleotides as described in the previous section. The complex was formed by combining 3×10^{-9} M Fl-$(dT)_{25}$ and 6×10^{-8} M DnaB helicase. The concentration of DnaB helicase was chosen so that the concentration of DnaB helicase was higher than the K_d. The decrease in anisotropy was monitored with an increase in competitor concentration, and data were analyzed by using a nonlinear least-square regression algorithm. The concentrations of unlabeled ligand required to displace half of the Fl-$(dT)_{25}$ from the complex (IC_{50}) were computed by nonlinear regression analysis. The inhibition constant K_i is given as

$$K_i = IC_{50}/(1 + R_T/K_d) \quad (11)$$

where R_T is the total concentration of Fl-$(dT)_{25}$. Since it is negligible compared to the K_d, the IC_{50} is equivalent to the inhibition constant, K_i.

RESULTS

DnaB helicase plays a pivotal role in chromosomal DNA replication in *E. coli* (*1*, *2*). Its donutlike hexameric structure is crucial to its mechanism of action, and this structure is a common feature of many DNA helicases (*34*). It should be noted that the mechanism of hexameric replicative DNA helicases as well as dimeric DNA helicases remains in the dark despite the advances in X-ray crystallographic structure determination of several of these helicases. It appears that the ssDNA binding as well as the ATP hydrolysis-dependent directional movement of the DNA helicase on ssDNA may have pivotal roles in the duplex DNA unwinding mechanism. Therefore, we have analyzed the mechanism and thermodynamics of equilibrium ssDNA binding by the DnaB helicase and the $DnaB_6$·$DnaC_6$ complex.

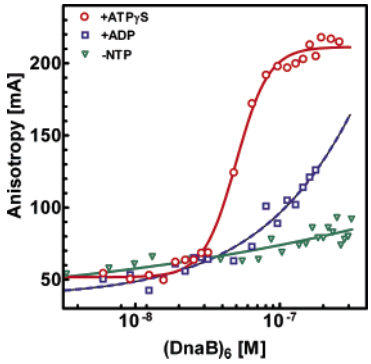

FIGURE 1: Effects of ATP and ADP on DnaB helicase−DNA interaction. Titration of 3 nM Fl-$(dT)_{25}$ with DnaB helicase at 23 °C. The fluorescence anisotropy was measured in the absence of nucleotide or in the presence of 100 μM nucleotide substrates ATPγS and ADP. Nonlinear regression fits were carried out using GraphPad Prism version 3.03 and are represented as lines.

Table 1: Nucleotide Modulation of the DnaB Helicase−ssDNA Interaction

nucleotide	$K_d \pm$ SD (M)	A_{min}	A_{max}	R^2
none	$\geq 4.65 \times 10^{-6}$	31	228	0.9041
ATPγS	$(5.09 \pm 0.32) \times 10^{-8}$	49	220	0.9928
ADP	$(2.08 \pm 0.31) \times 10^{-7}$	40	229	0.9642
GTP	$(3.17 \pm 0.53) \times 10^{-7}$	51	226	0.9453
CTP	$(3.75 \pm 0.27) \times 10^{-7}$	47	225	0.9793
dATP	$(1.07 \pm 0.22) \times 10^{-6}$	51	216	0.9141

DnaB Helicase Bound DNA with Moderate Affinity. We have quantitatively evaluated the interaction between DnaB and 5′-fluorescein-labeled, Fl-$(dT)_{25}$, in the presence and absence of various nucleotides. The fluorescence anisotropy of the free Fl-$(dT)_{25}$ was determined by using 3 nM oligonucleotide in buffer C containing 25 mM KCl. The anisotropy of free Fl-$(dT)_{25}$ was 47 ± 3 mA (Figure 1). The unbound Fl-$(dT)_{25}$ was then titrated with increasing concentrations of DnaB in a total volume of 1 mL at 23 °C. The anisotropy of the solution was measured ~5 min after each DnaB addition and mixing. Titrations were carried out in the absence and presence of 100 μM nonhydrolyzable ATP analogue, ATPγS or ADP. Preliminary studies (data not shown) indicate that a concentration of 100 μM for these nucleotides was optimal for fluorescence anisotropy analyses. A semilog plot of the anisotropy values at various DnaB concentrations gave rise to the binding isotherm shown in Figure 1. In the presence of 100 μM ATPγS, saturation of anisotropy was observed at 200 ± 10 mA. Nonlinear regression analysis of the data was used to determine apparent dissociation constants (K_d; eqs 2−9). The K_d for the DnaB helicase·Fl-$(dT)_{25}$ complex in the presence of ATPγS was $(5.09 \pm 0.32) \times 10^{-8}$ M (Figure 1 and Table 1).

The total fluorescence intensity during the measurement did not change significantly with an increase in DnaB helicase concentration. Therefore, the anisotropy values were not affected by the fluorescence lifetime changes or scattered excitation light. The DnaB hexamer can bind up to three oligonucleotides at very high oligonucleotide concentrations. However, in the DNA replication fork, it binds only one single strand. Under the conditions used in the anisotropy measurement of ssDNA binding, only one ssDNA molecule would bind per hexamer. Therefore, binding of other ssDNA molecules did not interfere with the measurements.

Nucleotide Modulation of Affinity and Specificity of DNA Binding. DNA binding by DnaB helicase was significantly modulated by adenine nucleotides (Figure 1). In the absence of nucleotides, very little change in anisotropy was observed, indicating a lack of ssDNA binding, and the K_d was $\geq 4.65 \times 10^{-6}$ M. Therefore, in the absence of nucleotides, DnaB did not bind ssDNA to a significant extent. In the presence of 100 μM ATP, the apparent K_d was $(1.17 \pm 0.25) \times 10^{-7}$ M, which was significantly lower than that observed with ATPγS. DnaB helicase is a potent DNA-dependent ATPase. Consequently, the concentration of ADP in the binding reaction was significant and increased during titration of DnaB. Therefore, the modulation of ssDNA binding by ATP alone could not be measured experimentally with any reasonable accuracy. On the other hand, ATPγS is a nonhydrolyzable analogue, and therefore, the measured ssDNA binding constant in the presence of ATPγS represents the formation of the DnaB·Fl-$(dT)_{25}$·ATPγS ternary complex in the complete absence of ADP. It is perhaps possible that the K_d of DNA binding in the presence of ATP is lower or the binding affinity is higher than that observed with ATPγS. However, experimentally, this is the equivalent condition where precise measurements of binding affinity or K_d are possible. A much lower affinity of DNA binding was observed in the presence of ADP. The K_d for the formation of the DnaB·Fl-$(dT)_{25}$·ADP ternary complex was $(2.08 \pm 0.31) \times 10^{-7}$ M (Figure 1 and Table 1). The dissociation constants for ssDNA binding in the presence of ADP and ATPγS appeared to be substantially different. The difference in the dissociation constants of DnaB−ssDNA binding suggests ATP-dependent ssDNA binding and ADP-dependent dissociation.

We have analyzed other nucleotides, GTP, CTP, and dATP, as cofactors for ssDNA binding (Figure 2 and Table 1). Both GTP and CTP increased the ssDNA binding affinity of DnaB helicase. However, both of these ribonucleotides were inferior to ATPγS (Figure 2 and Table 1). The least effective of the nucleotides was dATP (Figure 2D). The binding of ssDNA by the DnaB helicase required ribonucleotides.

Length and Sequence Specificity of DNA Binding by DnaB Helicase. The binding affinities of oligonucleotides of varying length and sequences were tested by competition analysis as described in Materials and Methods. The DnaB helicase·Fl-$(dT)_{25}$ complex was formed from DnaB helicase and Fl-$(dT)_{25}$, and the anisotropy of the complex was measured (Figure 3). Unlabeled oligonucleotides displaced Fl-$(dT)_{25}$ from the complex, and the anisotropy decreased due to the release of free Fl-$(dT)_{25}$ from the complex (Figure 3). At high competitor concentrations, anisotropy was reduced to ~42 mA which was equivalent to the anisotropy

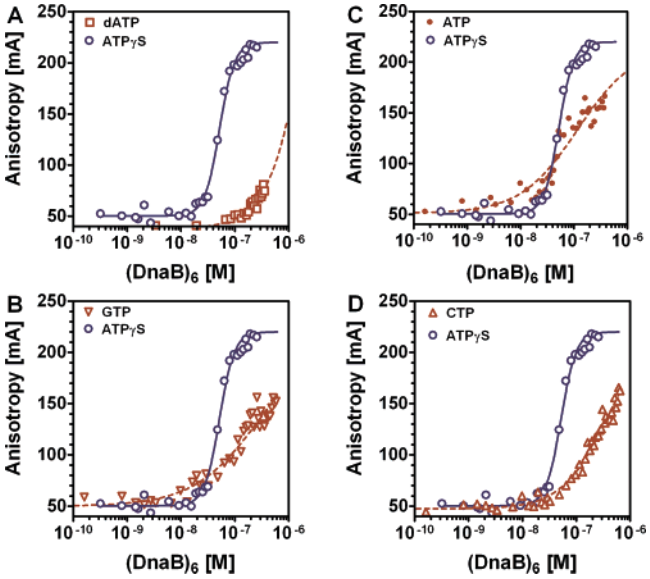

FIGURE 2: Effects of ribo- and deoxynucleotides on DnaB helicase−DNA interaction. The fluorescence anisotropy was measured in the presence of 100 μM nucleotide substrates ATPγS, ATP, CTP, GTP, and dATP. The buffer for each set of experiments consisted of 20 mM Tris-HCl (pH 7.5), 10% glycerol, and 25 mM KCl. Nonlinear regression fits are represented as lines.

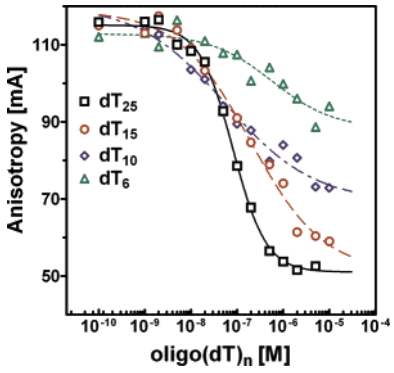

FIGURE 3: Inhibition of Fl-$(dT)_{25}$ binding by unlabeled oligonucleotides of different lengths and sequences. Titration of the preformed Fl-$(dT)_{25}$·DnaB helicase complex with competitor oligonucleotides $(dT)_{25}$, $(dT)_{15}$, $(dT)_{10}$, and $(dT)_6$. The temperature was held constant at 23 °C. The buffer consisted of 20 mM Tris-HCl (pH 7.5), 10% glycerol, 1 mM DTT, 5 mM Mg^{2+}, and 25 mM KCl. Nonlinear regression fits are represented as lines.

of free Fl-$(dT)_{25}$ as shown in Figure 2A. The anisotropy values obtained from the competitor titration were analyzed by nonlinear regression, and the inhibition constants (K_i) were determined (eq 10). The K_i value was $(5 \pm 0.6) \times 10^{-8}$ M for unlabeled oligo$(dT)_{25}$, which was comparable to the K_d value $(5.509 \times 10^{-8}$ M) of Fl-$(dT)_{25}$ binding (Table 1).

Competition analyses for oligo(dT) forms of varying lengths were carried out, and the data were analyzed by nonlinear least-square regression (Figure 3). In general, the apparent inhibition constants increased with a decrease in the length of the oligonucleotides. Both oligo$(dT)_{30}$ and oligo$(dT)_{20}$ demonstrated inhibition similar to that of oligo-$(dT)_{25}$, suggesting that the binding was independent of length above 20 bp (data not shown). The DNA binding affinity decreased with length below 20 bp. The inhibition constant for oligo$(dT)_{15}$ was 3-fold higher than that obtained for oligo-$(dT)_{25}$, whereas the K_i for oligo$(dT)_6$ was in the micromolar range. Our results demonstrated that the DNA binding

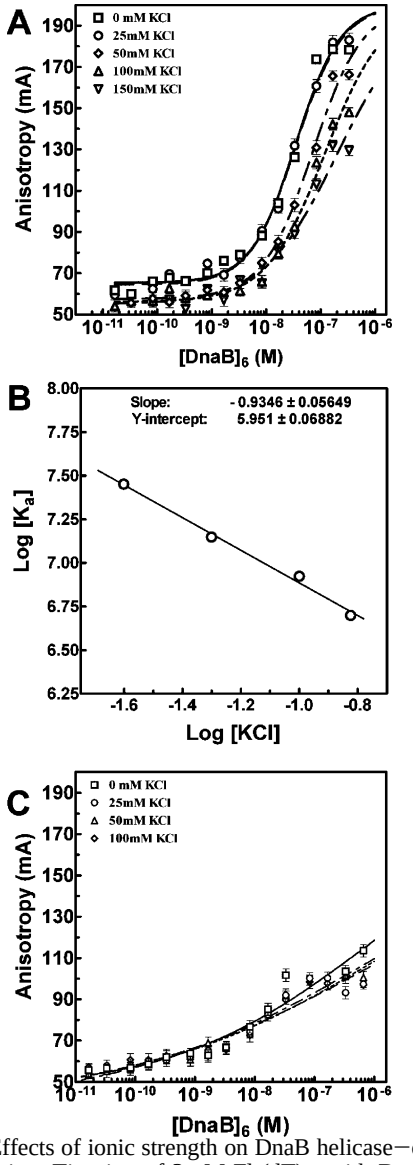

FIGURE 4: Effects of ionic strength on DnaB helicase−oligonucleotide interaction. Titration of 3 nM Fl-$(dT)_{25}$ with DnaB helicase at 23 °C. (A) In the presence of 100 μM ATPγS at KCl concentrations of 0, 25, 50, 100, and 150 mM. (B) Plot of log(K_a) vs log[KCl]. Linear regression analysis determined the slope and *Y*-intercept. (C) In the presence of 100 μM ADP at KCl concentrations of 0, 25, 50, and 100 mM. The buffer consisted of 20 mM Tris-HCl (pH 7.5), 10% glycerol, 1 mM DTT, and 5 mM Mg^{2+}. Lines represent nonlinear regression fits.

affinity of DnaB helicase depends on the length of the template, and it was optimal with ≥20 nucleotides. In addition, in the case of oligonucleotides with fewer than 10 nucleotides, more than one oligonucleotide molecule may bind to the same active sites. However, oligonucleotides are negatively charged molecules; as a result, ionic repulsion as well as van der Waals interactions may somewhat minimize this possibility of binding to a single site.

Modulation of DNA Binding by Ionic Strength. Protein−DNA interaction is often modulated by the ionic strength in solution, and this modulation is an indirect measure of the strength of ionic and hydrophilic interaction between the protein and DNA. Consequently, we have carried out binding studies at increasing salt concentrations: 0, 25, 50, 100, and 150 mM KCl. At 0 mM KCl, anisotropy of Fl-$(dT)_{25}$ increased as previously observed, at 25 mM KCl, with an increase in DnaB helicase concentration, and the binding isotherm demonstrated high-affinity ssDNA binding in the presence of ATPγS (Figure 4A and Table 2). The binding isotherms were shifted to higher protein concentrations with an increase in ionic strength. The dissociation constant at 0 mM KCl was 3.48×10^{-8} M, and it increased 5-fold to 2.0×10^{-7} M at 150 mM KCl (Table 2). The log(K_a) versus log[KCl] plot between 25 and 150 mM KCl indicated a linear dependence between K_d and KCl concentration (Figure 4B). In contrast, binding of DnaB to ssDNA in the presence of ADP was weak and did not change with ionic strength (Figure 4C and Table 2). Consequently, our results indicate that the DnaB and ssDNA interactions were fundamentally different in the presence of ATP and ADP.

Effects of Temperature on ssDNA Binding. To explore the thermodynamics of binding of DnaB helicase to DNA sequences, we have analyzed ssDNA binding at several different temperatures: 20, 25, 30, 32, 37, and 42 °C. The binding isotherms for binding of DnaB helicase to Fl-$(dT)_{25}$ with ATPγS and 25 mM KCl are presented in Figure 5. Saturation DNA binding was observed at all of these temperatures. The anisotropy of free and bound Fl-$(dT)_{25}$ also changed with temperature. Overall, anisotropy values of both free and bound DNA decreased with an increase in temperature, which was due to a decrease in the viscosity of the solution with an increase in temperature. Therefore, the anisotropy plots were normalized as shown in Figure 5. Following normalization of the data, it was clear that differences in isotherms at different temperatures were mostly ascribed to changes in the viscosity of the solution with temperature (Figure 5). The normalized plots (Figure 5 inset) indicated that there was no significant change in K_d with temperature in the 25−42 °C range, and the average K_d was $(5.2 \pm 1.53) \times 10^{-8}$ M. Below 25 °C, we observed a small decrease in K_d [$(2.88 \pm 0.4) \times 10^{-8}$ M] at 20 °C, which could be an indication of a small entropic contribution or hydrophobic interaction in the DNA binding. Results of the global analysis of the data also indicate that K_d remains constant above 25 °C (Table 3). The enthalpic contributions

Table 2: Changes in DnaB Helicase Dissociation Constants with Ionic Strength and Temperature

	0 mM salt	25 mM salt	50 mM salt	100 mM salt	150 mM salt
$K_{d[ATP\gamma S]} \times 10^8$ (M)	3.48 ± 0.53	3.54 ± 0.48	7.11 ± 0.71	11.94 ± 0.49	20 ± 0.69
$K_{d[ADP]} \times 10^7$ (M)	7.1 ± 6.5	21.5 ± 12	12.1 ± 7.6	19.6 ± 9.5	ND

Table 3: Changes in DnaB Helicase Dissociation Constants with Temperature[a]

	20 °C	25 °C	30 °C	35 °C	37 °C	42 °C
$K_{d[ATP\gamma S]} \times 10^8$ (M)	3.06 ± 0.56	7.79 ± 4.0	5.38 ± 2.5	4.49 ± 1.05	5.38 ± 2.1	4.27 ± 1.2

[a] The K_d values were derived from a direct global fitting analysis of the experimental data without normalization.

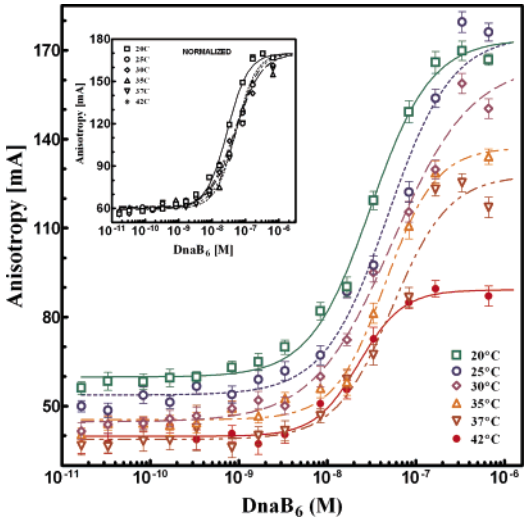

FIGURE 5: Temperature modulation of DnaB helicase−oligonucleotide interaction. Titration of 3 nM Fl-(dT)$_{25}$ with DnaB helicase and 100 μM ATPγS at 20, 25, 30, 35, 37, and 42 °C. The inset shows normalized anisotropy data for the titration of 3 nM Fl-(dT)$_{25}$ with DnaB helicase.

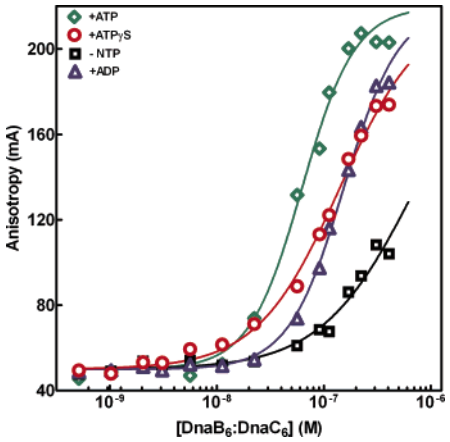

FIGURE 6: Nucleotide modulation of the DnaB−DnaC complex−ssDNA interaction. Fl-(dT)$_{25}$ (3 nM) was titrated with the DnaB·DnaC complex in either the absence of nucleotide or the presence of 100 μM ATPγS, ADP, or ATP. The temperature was held constant at 23 °C. The buffer consisted of 20 mM Tris-HCl (pH 7.5), 10% glycerol, 1 mM DTT, 5 mM Mg^{2+}, and 25 mM KCl. The data were analyzed by nonlinear regression analysis.

Table 4: Nucleotide Modulation of ssDNA Binding by the DnaB$_6$·DnaC$_6$ Complex

nucleotide	K_d (M)
none	$(7.23 \pm 0.26) \times 10^{-7}$
ATPγS	$(1.41 \pm 0.2) \times 10^{-7}$
ATP	$(6.26 \pm 0.65) \times 10^{-8}$
ADP	$(1.54 \pm 0.45) \times 10^{-7}$

from ionic and other noncovalent bonds are likely the major contributors to the stability of the DnaB−ssDNA complex.

Single-Stranded DNA Binding by the DnaB·DnaC Complex. The DnaB·DnaC complex was prepared using purified recombinant DnaB and DnaC proteins followed by gel filtration chromatography as described in Materials and Methods (*15*). The purified DnaB·DnaC complex was used for ssDNA binding studies. The DnaB·DnaC complex bound Fl-(dT)$_{25}$ in the absence of nucleotide cofactors with a lower affinity, and the K_d was 7.23×10^{-7} M (Figure 6 and Table 4). Unlike that of DnaB, high-affinity ssDNA binding was

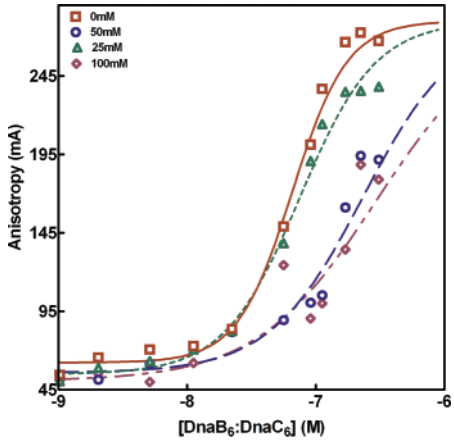

FIGURE 7: Effect of ionic strength on the DnaB−DnaC complex−ssDNA interaction. Fl-(dT)$_{25}$ (3 nM) was titrated with the DnaB·DnaC complex in the presence of 100 μM ATPγS in a buffer containing 20 mM Tris-HCl (pH 7.5), 10% glycerol, 1 mM DTT, 5 mM Mg^{2+}, and 0, 25, 50, or 100 mM KCl. The data were analyzed by nonlinear regression analysis.

observed only in the presence of ATP and not ATPγS. The binding affinity increased 10-fold in the presence of ATP with a K_d of 6.26×10^{-8} M. In the presence of ATPγS and ADP, the binding affinities were lower and K_d values were 1.41×10^{-8} and 1.54×10^{-8} M, respectively. ATP hydrolysis is significantly attenuated in the DnaB·DnaC complex (*7*, *15*). As a result, it is possible to measure the degree of ATP stimulation of ssDNA binding without significant interference from ADP. The binding affinity of the DnaB·DnaC complex for ssDNA in the presence of ATP was comparable to that of the DnaB hexamer in the presence of ATPγS.

Similar to that of the DnaB hexamer, the binding affinity of the DnaB·DnaC complex decreased with an increase in ionic strength (Figure 7). The highest-affinity ssDNA binding was observed between 0 and 25 mM KCl and weakened dramatically above 25 mM KCl. In the case of DnaB, the decrease in binding affinity was gradual with an increase in ionic strength, whereas with the DnaB·DnaC complex, a sharp change in K_d between 25 and 50 mM KCl was observed.

DISCUSSION

Unlike that for sequence specific DNA binding proteins such as transcription factors, DNA binding by the DnaB helicase is dynamic, mobile, and processive and lacks sequence specificity. Therefore, ssDNA binding by DnaB helicase is complex, and the thermodynamics of the binding remain unclear. Quantitative analyses of DnaB helicase−ssDNA interaction and the modulation by nucleotide cofactors were carried out by assessing equilibrium DNA binding to delineate the driving forces behind protein−DNA interaction.

Analysis of true equilibrium DNA binding by measuring changes in the fluorescence anisotropy of the ssDNA can provide detailed quantitative information about the thermodynamics of protein−DNA interaction. Titration of Fl-(dT)$_{25}$ with an increasing DnaB concentration produced sigmoidal binding isotherms as shown in Figure 1. Nonlinear regression analysis of the binding isotherms allowed for determination of the equilibrium binding constants. An inherent difficulty

Scheme 1: Conformational States of the DnaB Hexamer and Its Complexes

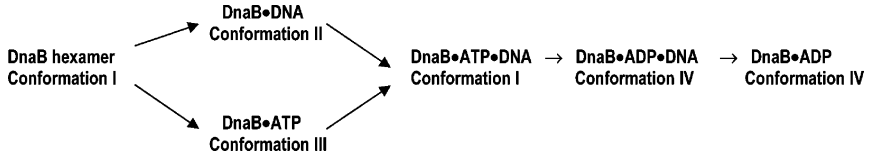

associated with these studies was due to the fact that DnaB helicase is a strong ATPase in the presence or absence of DNA ($1.7-6.0 \times 10^6$ pmol min^{-1} mg^{-1}). As a result, measurements of ssDNA binding in the presence of ATP were not possible because of the rapid conversion of ATP to ADP. The binding isotherm in the presence of ATP did not reach saturation, and the plots were highly variable (data not shown). Therefore, the measurements had to be carried out in the presence of a nonhydrolyzable analogue of ATP, ATPγS. In the presence of ATPγS, saturable binding was observed (Figure 1). The dissociation constant with ATPγS was $(5.09 \pm 0.32) \times 10^{-8}$ M, and it decreased significantly in the presence of ADP. The binding affinity of DnaB helicase for ssDNA changed with the nucleotide cofactor in the following order: ATP > ADP $\gg$ NTP.

A similar observation was made with other ribo- and deoxynucleotides (Figure 2). All of the nucleotides acted as positive effectors of ssDNA binding. dATP was less effective than the ribonucleotides. However, with none of the natural ribonucleotides was saturation binding observed. Saturation and high-affinity binding were observed only with nonhydrolyzable analogues such as ATPγS which likely mimicked the true effect of ATP without any interference from ADP. Even with GTP and CTP, hydrolysis to diphosphates remains a significant problem (*6*), and the higher-affinity binding similar to that observed with ATPγS was not detected.

This observation can be correlated to an opening or relaxation of the DnaB hexamer in the presence of ADP. Previously, we analyzed the structural effects of binding of DNA and nucleotide to DnaB helicase using tryptophan (Trp) fluorescence quenching with potassium iodide as a collisional quencher (*32*). The Trp fluorescence anisotropy of DnaB was measured in the presence and absence of ATP or ADP, to differentiate between dissociation and relaxation of the hexamer. The anisotropy of DnaB helicase was 260 ± 5 mA when it was bound to ATPγS and 275 ± 5 mA when it was bound to ADP. These results were found to be consistent with those obtained by San Martin et al. (*34*) from electron microscopic analysis of the DnaB hexamer in the presence of AMPPNP or ADP. Thus, it appears that in the DnaB·ssDNA·ADP ternary complex, the bound ssDNA may have a much higher degree of rotational movement due to relaxation of the hexamer and a relaxed mode of ssDNA binding. Our studies (*32*) involving fluorescence quenching analysis of the complex formation of DnaB hexamer with ssDNA and ATPγS or ADP, leading to a DnaB·ssDNA·ATPγS or DnaB·ssDNA·ADP complex, indicate that both DnaB·ssDNA·ADP and DnaB·ADP complexes have very open structures compared to the ATPγS-bound complexes. In the ADP-bound complexes, hydrophobic Trp moieties were more exposed to the solvent and quenchers than that observed with the DnaB hexamer alone or the DnaB·ssDNA·ATPγS complex. On the basis of the results of the Trp fluorescence quenching analysis (*32*), we identified four discreet conformational states of the DnaB hexamer, induced by the bound substrate or substrates, as shown in Scheme 1.

Conformation I is the most taut or closed conformation, whereas conformation IV is the most open or relaxed. The anisotropy results support the notion that conformation IV of the DnaB·ssDNA·ADP complex is an open and relaxed conformation with significant relaxation of ssDNA binding. Results presented here demonstrate that the ssDNA binding affinity of DnaB helicase is significantly attenuated in the presence of 100 μM ADP, concomitant with a relaxed structure, which agrees well with the binding model in Scheme 1. The results of the anisotropy studies described here indicate that the ATPγS-induced conformation in DnaB led to higher-affinity ssDNA binding and that the ADP-induced conformation led to lower-affinity binding. Therefore, each cycle of ATP hydrolysis likely leads to conformational changes in DnaB subunits, from conformation III to conformation I to conformation IV (Scheme 1), along with concomitant binding and release of ssDNA. Each step of these cycles contributes to the duplex DNA unwinding through this series of conformational changes as well as ssDNA binding and release.

The interaction between the ssDNA and DnaB helicase is multipartite. The change in free energy, $\Delta G°$, has enthalpic and entropic contributions ($\Delta G° = \Delta H° - T\Delta S°$). In the case of DnaB−ssDNA interaction, the entropic contribution appeared to be small. Temperature dependence studies (Figure 5) indicate that the K_d is relatively independent of temperature over a range of temperature from *X* to *Y*. Therefore, there is a small entropic contribution to the interaction, which is detectable in the lower temperature range (Figure 5). However, in large part, the DnaB−ssDNA−ATPγS interaction appeared to be enthalpy-driven, as the enthalpy change was the major component of the free energy change. In the presence of ATPγS, the interaction appeared to be highly dependent on ionic strength (Figure 4). These results also suggest that the interaction was substantially ionic and/or hydrophilic in nature in the presence of ATP. Although it is quite difficult to analyze the nature of the DnaB−ssDNA interaction in the presence of ADP due to the weak nature of the interaction (Figure 1), it is a distinct possibility that the enthalpic component or the ionic or hydrophilic component of the interaction was significantly reduced in the presence of ADP. Thus, the entropic contribution becomes the dominant part of the interaction in the presence of ADP, which is also justified by the fact that the K_d remained unaltered with an increase in ionic strength in the presence of ADP unlike that observed in the presence of ATP. Therefore, the entropic or hydrophobic interactions play an important role in maintaining a basal DnaB−ssDNA interaction. On the other hand, in the presence of ATP, additional ionic and hydrophilic interactions are formed that enhance the DnaB−ssDNA interaction, and these interactions are supported by the taut conformation of DnaB (Scheme 1). Consequently, when ATP is hydrolyzed to ADP and P_i, the ionic and hydrophilic interactions are disrupted and

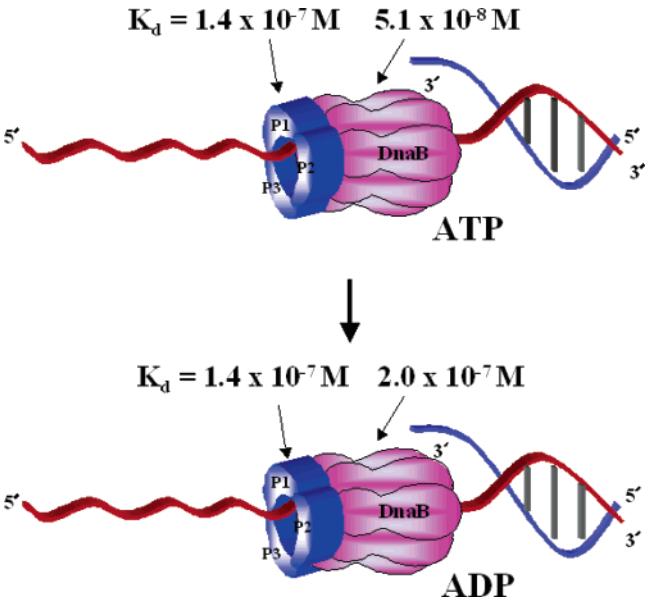

FIGURE 8: Interactions of the ssDNA template with the primase·DnaB complex. The cartoon represents the interaction of DnaB helicase and DnaG primase with ssDNA in the presence of ATP and ADP. The primase·DnaB complex is composed of three primase monomers and one DnaB hexamer (*36*). K_d values for the primase−ssDNA interaction and the DnaB−ssDNA interaction in the presence of ADP or ATP nucleotide cofactors are shown.

retracted in concert with the relaxation of DnaB from conformation I to IV. It is possible that during this step the ssDNA is released from one of the DNA binding sites, is twisted, and moves to the spatially next binding site (*35*).

Previously, we have studied the interaction between *E. coli* DNA primase and ssDNA (*23*). Unlike DnaB−ssDNA interaction, primase−ssDNA interaction is found to be largely entropy driven, which is strongly influenced by temperature changes and is relatively independent of the ionic strength of the reaction (*23*). The primase−ssDNA interaction is weak, and the K_d is 1.4×10^{-7} M. This value of K_d is comparable to the K_d of DnaB−ssDNA interaction in the presence of ADP. Therefore, in the ADP-bound state, the primase·DnaB complex, consisting of three primase monomers and one DnaB hexamer, would interact with the ssDNA at both the primase site and the DnaB site with comparable binding affinities (Figure 8). When ATP displaces ADP in the DnaB binding site, the binding at the DnaB site would change and switch to high-affinity binding, whereas the binding affinity of the primase site should remain unaltered. Together, these two binding sites allow simultaneous unwinding and RNA primer synthesis by the same DnaB·primase assembly.

Unlike the DnaB hexamer, the preformed $DnaB_6$·$DnaC_6$ complex is absolutely required ATP for high-affinity DNA binding. Neither ATPγS nor ADP could substitute for ATP, and thus, ATP hydrolysis appeared to be a prerequisite of high-affinity ssDNA binding by the $DnaB_6$·$DnaC_6$ complex (Figure 6). As the complex hydrolyzes ATP at a slow rate and ADP significantly lowers the DNA binding affinity, the true K_d in the presence of ATP is likely lower than the observed K_d of $(6.26 \pm 0.65) \times 10^{-8}$ M (Figure 6 and Table 3). It should be noted that our earlier studies indicated that formation of a complex between DnaB helicase and DnaC protein does not require nucleotides [$K_d = (3.5 \pm 0.01) \times 10^{-7}$ M] and nucleotides actually inhibit complex formation [$K_{d,ADP} = (28 \pm 0.03) \times 10^{-7}$ M] (*13*). However, the inhibition is eliminated in the presence of oligo(dT)$_{25}$ and ATP [$K_d = (2.6 \pm 0.02) \times 10^{-7}$ M]. Once ATP is hydrolyzed to ADP, the K_d of complex formation increases 15-fold [$K_d = (39 \pm 0.09) \times 10^{-7}$ M]. Therefore, a spontaneous dissociation of the ssDNA·$DnaB_6$·$DnaC_6$·ADP complex with the release of DnaC is most probable. Consequently, the DnaB·DnaC complex will bind DNA with high affinity in the presence of ATP; however, upon hydrolysis to ADP, the ssDNA·$DnaB_6$·$DnaC_6$·ADP complex will dissociate to the ssDNA·DnaB·ADP complex rapidly, and the cycle of ATP binding, hydrolysis, and DNA binding and unwinding will begin as shown in Scheme 2.

Scheme 2: Nucleotide Regulation of ssDNA Binding by the DnaB·DnaC Complex

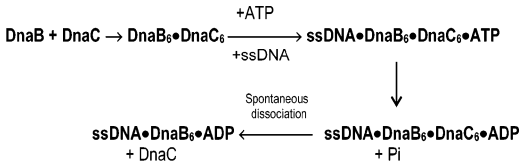

ACKNOWLEDGMENT

We thank Dr. Joseph R. Lakowicz from the University of Maryland School of Medicine (Baltimore, MD) for making instruments available for anisotropy measurementsm and Dr. Catherine A. Royer from the Centre de Biochimie Structurale (INSERM, Montpellier, France) for the gift of BIOEQS software for fluorescence data analysis and training involving use of the software.

REFERENCES

1. Kornberg, A., and Baker, T. A. (1992) *DNA Replication*, W. H. Freeman and Co., New York.
2. LeBowitz, J. H., and McMacken, R. (1986) The *Escherichia coli* dnaB replication protein is a DNA helicase, *J. Biol. Chem. 261*, 4738−4748.
3. Bramhill, D., and Kornberg, A. (1988) A model for initiation at origins of DNA replication, *Cell 54*, 915−918.
4. Kornberg, A. (1987) Enzyme systems initiating replication at the origin of the *Escherichia coli* chromosome, *J. Cell Sci., Suppl. 7*, 1−13.
5. Arai, K., Yasuda, S., and Kornberg, A. (1981) Mechanism of dnaB protein action. I. Crystallization and properties of dnaB protein, an essential replication protein in *Escherichia coli*, *J. Biol. Chem. 256*, 5247−5252.
6. Arai, K., and Kornberg, A. (1981) Mechanism of dnaB protein action. II. ATP hydrolysis by dnaB protein dependent on single- or double-stranded DNA, *J. Biol. Chem. 256*, 5253−5259.
7. Biswas, E. E., Biswas, S. B., and Bishop, J. E. (1986) The dnaB protein of *Escherichia coli*: Mechanism of nucleotide binding, hydrolysis, and modulation by dnaC protein, *Biochemistry 25*, 7368−7374.
8. Patel, S. S., and Hingorani, M. M. (1993) Oligomeric structure of bacteriophage T7 DNA primase/helicase proteins, *J. Biol. Chem. 268*, 10668−10675.
9. Patel, S. S., and Picha, K. M. (2000) Structure and function of hexameric helicases, *Annu. Rev. Biochem. 69*, 651−697.
10. Raney, K. D., and Benkovic, S. J. (1995) Bacteriophage T4 Dda helicase translocates in a unidirectional fashion on single-stranded DNA, *J. Biol. Chem. 270*, 22236−22242.
11. Raney, K. D., Carver, T. E., and Benkovic, S. J. (1996) Stoichiometry and DNA unwinding by the bacteriophage T4 41:59 helicase, *J. Biol. Chem. 271*, 14074−14081.

12. Biswas, E. E., Chen, P. H., and Biswas, S. B. (2002) Modulation of enzymatic activities of *Escherichia coli* DnaB helicase by single-stranded DNA-binding proteins, *Nucleic Acids Res. 30*, 2809−2816.
13. Biswas, S. B., Flowers, S., and Biswas-Fiss, E. E. (2004) Quantitative analysis of nucleotide modulation of DNA binding by DnaC protein of *Escherichia coli*, *Biochem. J. 379*, 553−562.
14. Davey, M. J., Fang, L., McInerney, P., Georgescu, R. E., and O'Donnell, M. (2002) The DnaC helicase loader is a dual ATP/ADP switch protein, *EMBO J. 21*, 3148−3159.
15. Kobori, J. A., and Kornberg, A. (1982) The *Escherichia coli* dnaC gene product. III. Properties of the dnaB-dnaC protein complex, *J. Biol. Chem. 257*, 13770−13775.
16. Kobori, J. A., and Kornberg, A. (1982) The *Escherichia coli* dnaC gene product. II. Purification, physical properties, and role in replication, *J. Biol. Chem. 257*, 13763−13769.
17. Biswas, S. B., and Biswas, E. E. (1987) Regulation of dnaB function in DNA replication in *Escherichia coli* by dnaC and λ P gene products, *J. Biol. Chem. 262*, 7831−7838.
18. LeBowitz, J. H., and McMacken, R. (1984) The bacteriophage λ O and P protein initiators promote the replication of single-stranded DNA, *Nucleic Acids Res. 12*, 3069−3088.
19. Learn, B. A., Um, S. J., Huang, L., and McMacken, R. (1997) Cryptic single-stranded-DNA binding activities of the phage λ P and *Escherichia coli* DnaC replication initiation proteins facilitate the transfer of *E. coli* DnaB helicase onto DNA, *Proc. Natl. Acad. Sci. U.S.A. 94*, 1154−1159.
20. Jezewska, M. J., and Bujalowski, W. (1996) A general method of analysis of ligand binding to competing macromolecules using the spectroscopic signal originating from a reference macromolecule. Application to *Escherichia coli* replicative helicase DnaB protein nucleic acid interactions, *Biochemistry 35*, 2117−2128.
21. Jezewska, M. J., and Bujalowski, W. (1996) Global conformational transitions in *Escherichia coli* primary replicative helicase DnaB protein induced by ATP, ADP, and single-stranded DNA binding. Multiple conformational states of the helicase hexamer, *J. Biol. Chem. 271*, 4261−4265.
22. Jezewska, M. J., Kim, U. S., and Bujalowski, W. (1996) Binding of *Escherichia coli* primary replicative helicase DnaB protein to single-stranded DNA. Long-range allosteric conformational changes within the protein hexamer, *Biochemistry 35*, 2129−2145.
23. Khopde, S., Biswas, E., and Biswas, S. (2002) Affinity and sequence specificity of DNA binding and site selection for primer synthesis by *Escherichia coli* primase, *Biochemistry 41*, 14820−14830.
24. LeTilly, V., and Royer, C. A. (1993) Fluorescence anisotropy assays implicate protein-protein interactions in regulating trp repressor DNA binding, *Biochemistry 32*, 7753−7758.
25. Royer, C. A., and Beechem, J. M. (1992) Numerical analysis of binding data: Advantages, practical aspects, and implications, *Methods Enzymol. 210*, 481−505.
26. Gryczynski, I., Steiner, R. F., and Lakowicz, J. R. (1991) Intensity and anisotropy decays of the tyrosine calmodulin proteolytic fragments, as studied by GHz frequency-domain fluorescence, *Biophys. Chem. 39*, 69−78.
27. Boyer, M., Poujol, N., Margeat, E., and Royer, C. A. (2000) Quantitative characterization of the interaction between purified human estrogen receptor α and DNA using fluorescence anisotropy, *Nucleic Acids Res. 28*, 2494−2502.
28. Royer, C. A., Smith, W. R., and Beechem, J. M. (1990) Analysis of binding in macromolecular complexes: A generalized numerical approach, *Anal. Biochem. 191*, 287−294.
29. Maleki, S. J., Royer, C. A., and Hurlburt, B. K. (2002) Analysis of the DNA-binding properties of MyoD, myogenin, and E12 by fluorescence anisotropy, *Biochemistry 41*, 10888−10894.
30. Ozers, M. S., Hill, J. J., Ervin, K., Wood, J. R., Nardulli, A. M., Royer, C. A., and Gorski, J. (1997) Equilibrium binding of estrogen receptor with DNA using fluorescence anisotropy, *J. Biol. Chem. 272*, 30405−30411.
31. Biswas, E. E., Chen, P. H., and Biswas, S. B. (1995) Overexpression and rapid purification of biologically active yeast proliferating cell nuclear antigen, *Protein Expression Purif. 6*, 763−770.
32. Flowers, S., Biswas, E. E., and Biswas, S. (2003) Conformational Dynamics of DnaB helicase upon DNA and Nucleotide Binding: Analysis by Intrinsic Tryptophan Fluorescence Quenching. *Biochemistry 42*, 1910−1921.
33. Lakowicz, J. R. (1999) *Principles of fluorescence spectroscopy*, 2nd ed., Plenum Publishers, New York.
34. San Martin, M. C., Stamford, N. P., Dammerova, N., Dixon, N. E., and Carazo, J. M. (1995) A structural model for the *Escherichia coli* DnaB helicase based on electron microscopy data, *J. Struct. Biol. 114*, 167−176.
35. Biswas, E. E., and Biswas, S. B. (1999) Mechanism of DNA binding by the DnaB helicase of *Escherichia coli*: Analysis of the roles of domain γ in DNA binding, *Biochemistry 38*, 10929−10939.
36. Mitkova, A. V., Khopde, S. M., and Biswas, S. B. (2003) Mechanism and stoichiometry of interaction of DnaG primase with DnaB helicase of *Escherichia coli* in RNA primer synthesis, *J. Biol. Chem. 278*, 52253−52261.

BI060118D